Developmental Morphology of Branchiomeric Nerves in a Cat Shark, Scyliorhinus torazame, with Special Reference to Rhombomeres, Cephalic Mesoderm, and Distribution Patterns of Cephalic Crest Cells

Authors: Kuratani, Shigeru, and Horigome, Naoto

Source: Zoological Science, 17(7) : 893-909

Published By: Zoological Society of Japan

URL: https://doi.org/10.2108/zsj.17.893

ZOOLOGICAL SCIENCE **17**: 893–909 (2000)

Developmental Morphology of Branchiomeric Nerves in a Cat Shark, *Scyliorhinus torazame*, with Special Reference to Rhombomeres, Cephalic Mesoderm, and Distribution Patterns of Cephalic Crest Cells

Shigeru Kuratani* and Naoto Horigome

Department of Biology, Faculty of Science, Okayama University
3-1-1 Tsushimanaka, Okayama 700-8530, Japan

ABSTRACT—Peripheral nerve development was studied in the cat shark, *Scyliorhinus torazame*, using whole-mount and sectioned embryos. Nerve fibers were immunohistochemically stained using a monoclonal antibody against acetylated tubulin and, in early embryos, cephalic crest cells were observed by scanning electron microscopy. The initial distribution patterns of crest cells were identical to the typical vertebrate embryonic pattern, in that three crest cell populations were associated with even-numbered rhombomeres, prefiguring the pattern of the branchiomeric nerve roots. In older pharyngula, however, the trigeminal and postotic branchiomeric nerve roots were found to have shifted caudally along the neuraxis: the trigeminal nerve root finally arose from r3, while the glossopharyngeal nerve root arose from the presumptive region r7 of the hindbrain. The shift apparently takes place between the root fibers and the dorsolateral fasciculus. From observing the topographical relationships between the peripheral nerves and other epithelial structures (for example, the otocyst and the mesodermal head cavities - the anlagen of extrinsic ocular muscles), it was assumed that the shift was the result of an epigenetic effect caused by allometric growth of the otocyst, the mandibular cavity, and the spiracle epithelia anchoring the mandibular branch of the trigeminal nerve. It was concluded that the deviated morphological pattern of elasmobranch cranial nerves is a secondary phenomenon caused by the well-developed head cavities. In those animals whose head cavities are degenerated, the original pattern of the cranial nerve-rhombomere assignment, which is intact in lamprey embryos, is retained.

INTRODUCTION

Among extant vertebrates, elasmobranchs are generally regarded as an outgroup to all other gnathostomes. Comprised of sharks and rays, the Elasmobranchs are characterized by unossified skeletons, odontoid scales in the skin, and a low grade of morphological differentiation of the pharyngeal arches (reviewed by Mallat, 1996). The eggs of oviparous species contain a large yolk and, by the pharyngula stage, the embryos attain a comparatively large size for vertebrates. For this reason, as well as their phylogenetic position, elasmobranch embryos have been extensively studied by comparative embryologists. These studies established the basic concept of the segmental organization of the vertebrate head (Balfour, 1878; van Wijhe, 1882; Dohrn, 1888; Goodrich, 1918; de Beer, 1922, 1937; reviewed by Goodrich, 1930; Bjerring, 1971, 1977; Jarvik, 1980; and Jefferies, 1986).

* Corresponding author: Tel. +81-86-251-7867;
FAX. +81-86-251-7876.
E-mail: sasuke@cc.okayama-u.ac.jp

A unique aspect of the elasmobranch embryo is the appearance of conspicuous head cavities, with transient epithelial mesoderm appearing in the head region (Balfour, 1878; van Wijhe, 1882; Scammon, 1911; Bjerring, 1971, 1977; reviewed by Jefferies, 1986; E. Gilland, personal communication). Similar cavities have been recognized in a number of vertebrate embryos, including those of amniotes, and they are believed to represent the primordia of extrinsic eye muscles (Brachet, 1935). Generally, the mesoderm in the head region develops three pairs of epithelialized pouches, the premandibular, mandibular, and hyoid cavities, or somites (Marshall, 1881; Lamb, 1902; Platt, 1891; Neal, 1918a,b; reviewed by Goodrich, 1930; Neal and Rand, 1942; de Beer, 1937; Starck, 1963; Jarvik, 1980; and Jefferies, 1986). The most rostral premandibular cavity is connected to its counterpart by a median bridge near the rostral tip of the notochord. In a few species, there is also an additional head cavity found more rostral than the premandibular cavity, known as Platt's vesicle (Platt, 1891). These three or four cavities were once thought to represent head mesomeres (mesodermal segments). Thus, the vertebrate head was assumed to originally

Table 1. Staging list of *S. torazame* embryos.

body lengths (mm)	post-oviposition age (days)	stages
3.5#	19	I
3.5#	19	
3.5#	22	II
3.5#	22	
8.0	– *	III
8.0	–	
9.5	–	IV
13.0	–	
14.0	–	
16.0	49	V
17.0	–	
17.5	49	
20.0	53	VI
20.0	–	
22.0	64	
22.0	–	
27.0	–	VII**
27.0	78	
32.0	107	

net growth is compensated between these stages due to the development of the cephalic flexure.
* "–" means no record.
** not described in the present study.

consist of three or four preotic segments (reviewed by Goodrich, 1930; de Beer, 1937; Neal and Rand, 1942; Jarvik, 1980; and Jefferies, 1986). The presence of these segmental mesodermal components is a curious problem for modern biology, since the theory of head segmentation has gained support through molecular studies (reviewed by Kuratani *et al.*, 1999). Thus, the development of the shark should be re-evaluated with techniques that were unavailable to the classical embryologists.

Segmental patterning of the embryonic head is not restricted to mesodermal elements. In the embryos of several gnathostomes, as well as in lampreys, the first three branchiomeric nerves primarily arise from even-numbered rhombomeres as a result of the selective association of crest cells with those rhombomeres (Kuratani *et al.*, 1997; Horigome *et al.*, 1999 and references therein). Regardless of such features, which may be ancestral, late pharyngula elasmobranch embryos exhibit a peculiar feature in their cranial nerve patterning. The trigeminal and facial nerve roots arise very close to each other on the hindbrain, such that the trigeminal nerve root appears to be placed too posteriorly (typically observed in 13-mm *Squalus acanthias*; Neal, 1914; see below). In the present paper, we chose to study the cat shark (*Scyliorhinus torazame*), whose eggs are easiest to collect in Japan. Histological and immunohistochemical methods were used to observe the staged development (Table 1) of the morphology of embryonic peripheral nerves to elucidate the apparently inconsistent cranial nerve configuration specific to this animal group. We also aimed to re-evaluate the morphology of elasmobranch embryos in the context of vertebrate head segmentation.

MATERIALS AND METHODS

Whole-mount immunostaining

Embryos of *S. torazame* (a gift from Marine World Umino-Nakamichi, Fukuoka, Japan) were brought into the laboratory and kept in sea water at 15°C. Embryonic stages were determined according to body lengths, which were consistent with the post-oviposition age (Table 1). Embryos were prepared as previously described (Kuratani *et al.*, 1997) with minor modifications. After fixation with 4% paraformaldehyde in 0.1% phosphate-buffered saline (PFA/PBS; containing 3% NaCl to adjust osmolarity) at 4°C for 1 day, embryos were washed in 0.9% NaCl in distilled water, dehydrated in a graded series of methanol solutions (50%, 80%, 100%) and stored at –20°C. The samples to be stained were placed on ice in 2 ml of dimethyl sulfoxide (DMSO)/methanol (1:1) until they sank. Then 0.5 ml of 10% Triton X-100/distilled water was added, and the embryos were incubated for an additional 30 min at room temperature. After washing in Tris-HCl-buffered saline (TST: 20 mM Tris-HCl, pH 8.0, 150 mM NaCl, 0.1% Triton X-100), the samples were sequentially blocked using aqueous 1% periodic acid and 5% non-fat dried milk in TST (TSTM).

A monoclonal antibody (mAb) raised against acetylated tubulin (monoclonal anti-acetylated tubulin, No. T-6793, Sigma Chemical Co., St. Louis, MO) was used to stain the cranial nerves. Embryos were incubated in the primary antibody (diluted 1/1,000 in spin-clarified TSTM containing 0.1% sodium azide) for 2 to 4 days at room temperature while being gently agitated on a shaking platform. Horseradish peroxidase (HRP)-conjugated goat anti-mouse IgG (ZYMED Lab. Inc., San Francisco, CA) diluted 1/200 in TSTM served as the secondary antibody. After a final washing in TST, the embryos were pre-incubated with the peroxidase substrate, 3,3'-diaminobenzidine (DAB, 100 μg/ml), in TST for 1 h and then allowed to react for 20 to 40 min at 0°C in TST with the same concentration of DAB also containing 0.01% (v/v) hydrogen peroxide (35% aqueous solution). The reaction was stopped, and the embryos were simultaneously clarified, by addition of 30% glycerol in 0.5% KOH. The stained embryos were transferred to 60% glycerol/water for observation. Line drawings were prepared based on photographs. Norris and Hughes (1920), Tanaka (1976, 1979), Tanaka and Nakao (1979), Northcutt (1993, 1997) and Northcutt and Brändle (1995) were consulted for anatomical terms.

Immunostaining of sectioned specimens

Specimens, fixed in Bouin's fixative (containing 3% NaCl to adjust osmolarity), were embedded in paraffin and sectioned at 5 μm. The sections were then deparaffinized, treated with 1% periodic acid for 5 min at room temperature, and washed in TST. Anti-acetylated tubulin (diluted 1/1,000) and anti-HNK-1 mAbs (Leu-7, Becton Dickinson, San Jose, CA; diluted 1/50) were used to label the developing nervous system on the paraffin-sectioned specimens. Primary antibodies were diluted in TSTM and applied to the sections for 1.5 h at room temperature. After washing with TST, the respective secondary antibodies, HRP-anti mouse IgG and IgM (ZYMED Lab. Inc.), were diluted 1/200 in TSTM and applied to the specimens for 40 min. After the peroxidase reaction, the sections were counter-stained with either cresyl violet or hematoxylin.

Scanning Electron Microscopy

Embryos, fixed in 2.5% glutaraldehyde/0.01 M phosphate buffer (PB: pH 7.6), were post-fixed with 4% osmium tetroxide. The specimens were then rinsed in PB, where they were also skinned with a sharpened tungsten needle. They were then dehydrated in a graded series of ethanol solutions and freeze-dried in *t*-butyl alcohol. Finally, the embryos were placed on an aluminum stub, sputter-coated with gold-palladium alloy, and viewed by scanning electron microscopy

(SEM; JSM-5800, JEOL).

Abbreviations

ac	anterior commissure
adllpl	anterodorsal lateral line placode
BC	branchial crest cells
BC(IX)	rostral subpopulation of branchial crest cells differentiating into the glossopharyngeal nerve anlage
blo	olfactory bulb
br1-5	branchial arches 1 to 5
cp	posterior commissure
del	endolymphatic duct
dlf	dorsolateral fasciculus
dm	dermomyotome
dvdt	dorsoventral diencephalic tract
epi	epiphysis
exn	external nostril
fb	forebrain
glall	preotic lateral line ganglion
glcil	ciliary ganglion
hb	hindbrain
HC	hyoid crest cells
HC(VII+VIII)	subpopulation of hyoid crest cells forming the acusticofacial nerve complex
hy	hyoid arch
hyc	hyoid cavity
hym	hyoid mesoderm
hyp	hypophysis
hypt	hypothalamus
I	olfactory nerve
III	oculomotor nerve
IV	trochlear nerve
IX	glossopharyngeal nerve
ln	lens
ma	mandibular arch
mb	midbrain
MC	trigeminal crest cells
mlf	medial longitudinal fasciculus
mnc	mandibular cavity
nt	notochord
olep	olfactory epithelium
opm	oropharyngeal membrane
os	optic stalk
ot	otic vesicle or otic pit
ov	optic vesicle
pf	pectoral fin bud
pll	posterior lateral line placode
poc	postoptic commissure
pp1-4	pharyngeal pouches or slits 1 to 4
prc	pericardium
prcpl	prechordal plate
prmc	premandibular cavity
prmx	maxillary prominence
r1-6	rhombomeres 1 to 6
rb	buccal nerve
rdsp1	dorsal branch of the first spinal nerve
rhmVII	hyomandibular branch of the facial nerve
rmandV23	mandibular branch of the maxillomandibular nerve
rmxV23	maxillary branch of the maxillomandibular nerve
rophs	superficial ophthalmic branch of the preotic lateral line nerve
rptIX	posttrematic branch of the glossopharyngeal nerve
rptX1-2	posttrematic branches of X1 and of X2
rsoV23	supraoptic branch of the trigeminal nerve
rvsp	ventral rami of spinal nerves
som	somites
sot	supraoptic tract
sp	spiracle
sp1	spinal nerve 1
spc	spinal cord
spd	spinal dorsal root
tac	tract of anterior commissure
TC	trigeminal crest cells
TC(V)	trigeminal crest cell subpopulation representing trigeminal nerve anlage
tel	telencephalon
thc	tract of the habenular commissure
tpoc	tract of the postoptic commissure
tra	truncus arteriosus of the heart
trMesV	mesencephalic trigeminal tract
uc	umbilical cord
V	trigeminal nerves or root
V1	ophthalmic profundus nerve
V23	maxillomandibular nerve
VI	abducens nerve
VII+VIII	acusticofacial nerve root
VIII	acoustic nerve
X	vagus nerve
XII	hypoglossal nerve

RESULTS

Stage I (19-day or 3.5-mm embryos)

The stage I *S. torazame* embryo appears similar to the stage F *Scyllium* embryo (Goodrich, 1918), corresponding to the early pharyngula. It exhibits two rostral pharyngeal pouches (Fig. 1A, B). The neural tube of the embryo contains a large optic vesicle and at this stage has formed a slight cephalic flexure at the level of the future midbrain. In the hindbrain, a pair of clear neuromeric boundaries can be seen. These represent the rostral and caudal boundaries of rhombomere 3 (r3).

Although at this stage, whole-mount immunostaining with the anti-acetylated tubulin mAb reveals no neurites, the anti-HNK-1 mAb specifically binds to an epithelial mesodermal pouch, located between the optic vesicle and the first pharyngeal pouch. This mesoderm will later become the mandibular head cavity (Fig. 1B). Consistent with earlier reports on elasmobranch embryos (Scammon, 1911; reviewed in Jefferies, 1986), histological sections reveal that this cavity arises as a typical enterocoel grown from the endodermal foregut. This antibody does not label neural crest cells.

Stage II (22-day or 3.5-mm embryos)

By stage II, overt cephalic crest cells can be recognized by SEM. Three putative crest cell populations are found in the embryo (Fig. 1C, D). These cells are superficially located in the head region and are easily distinguished from the more deeply embedded mesodermal cells. This implies a dorsolateral developmental pathway, characteristic of cephalic crest cells from embryos of other vertebrates. The overall morphology and crest cell distribution show a similarity to the stage G *Scyllium* embryo described by Goodrich (1918). In S. *torazame* at this stage, rhombomeric boundaries can be seen at the levels of r1/2, r2/3, r3/4, r4/5 and r5/6, but the mid-hindbrain

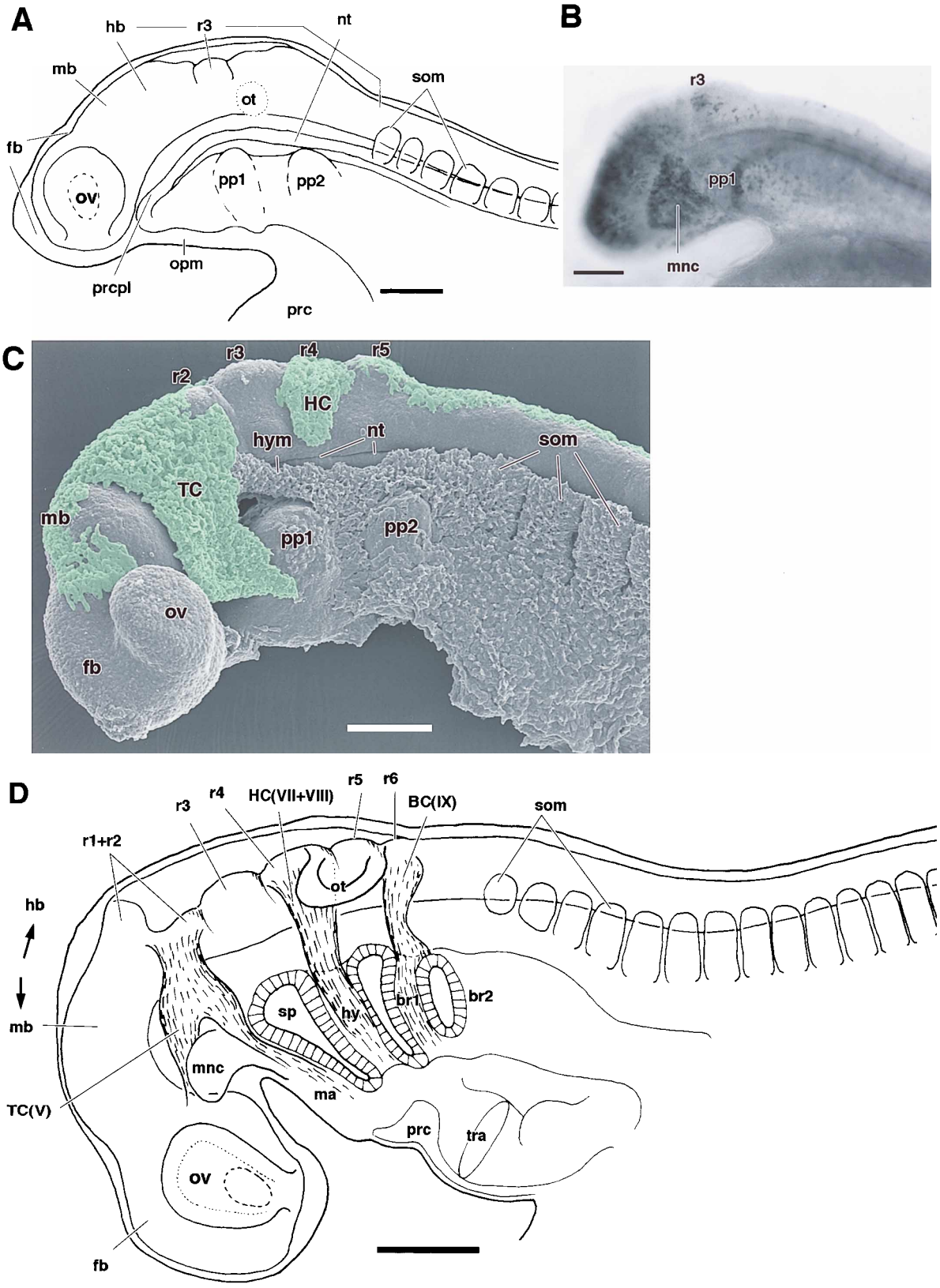

boundary is not detectable (Fig. 1D). Each crest population is associated with a particular rhombomere. The most rostral and largest cell population, the trigeminal crest cells, covers the anterior part of the neural tube rostral to the r2/3 boundary. The second cell population, the hyoid crest cells, adheres to r4. The most caudal cell population, the branchial crest cells, has just begun emigration from the neural tube at the level of r5 or more caudally. No crest cells are seen on the surface of r3 (Fig. 1C, D). The trigeminal crest cells have already migrated into the mandibular arch and premandibular regions. It is not clear whether the absence of crest cells from the lateral aspect of the midbrain is an artefact of preparation, or whether it reflects the normal distribution pattern of crest cells in this species at this stage. However, in the 3.5-mm embryo of *Squalus acanthias*, a crest cell-free space in the same region divides trigeminal crest cells into two sub-populations: trigeminal crest cells posteriorly and thalamic crest cells anteriorly (Scammon, 1911). In either case, crest cells rapidly fill this space during subsequent stages (see below).

No acetylated tubulin immunoreactivity is observed in any neurites at this stage. Nonetheless, observation of the whole-mount embryo enables us to distinguish three compact streams of crest cells representing the initial primordia of three branchiomeric nerves (the trigeminal, acusticofacial and glossopharyngeal nerves; Fig. 1D). As seen in several other vertebrate embryos, each cranial nerve primordium is associated with an even-numbered rhombomere, with the exception of the vagal nerve primordium, which cannot be detected at this stage.

At the dorsal aspect of the mandibular cavity, the cell stream representing the trigeminal nerve anlage bifurcates into two substreams, representing the profundal and maxillomandibular divisions, respectively (Fig. 1D). Of the two divisions, the latter penetrates into a narrow space between the caudal surface of the mandibular cavity and the rostral aspect of the first pharyngeal pouch. Similar topographical relationships have been described in the stage K *Galeus canis* embryo by van Wijhe (1882) and in the 4.5-mm *Squalus acanthias* embryo by de Beer (1922).

Stages III and IV (8.0- to 9.5-mm embryos)

Cephalic crest cell populations exhibit the typical vertebrate pattern at stage III. This is similar to the 5-mm *Torpedo* embryo described by Froriep (1905) and the 8-mm *Squalus* acanthias embryo described by de Beer (1922). Trigeminal crest cells cover the entire area innervated by the trigeminal nerve, including the mandibular arch, the premandibular (infraoptic) regions, the cavum epiptericum, and the supraoptic region. Hyoid crest cells extend from r4 to the hyoid arch, and the postotic pharyngeal arches are entirely covered by branchial crest cells (Fig. 2A). Proximally, each crest cell population maintains a relationship with its respective rhombomere similar to that seen during the previous stage, except that the cells appear to have been excluded from r5, thereby leaving two crest cell-free spaces lateral to r3 and r5. In addition, when compared with stage II, there is a caudal shift in the relative position of the branchial crest cells associated with the growth of the otocyst (see below).

The epiphysis and telencephalon first begin to emerge in the forebrain at stage IV (Fig. 2B); this roughly corresponds to the 10-mm stage of *Scyllium* (Goodrich, 1918). At this point, whole-mount immunostaining of neurites becomes possible, and a significant change is observed in the position of the branchiomeric nerve primordia: the trigeminal nerve root is now found on the rostral portion of r3 (Fig. 2B). Distally, trigeminal nerve branches show a growth pattern analogous to that of the trigeminal crest cell streams at stage II (Fig. 1D). The profundal nerve passes dorsal to the aspect of the mandibular cavity, and the maxillomandibular branch passes ventrally between the caudal aspect of the mandibular cavity and the rostral wall of the spiracle (Fig. 2B). The mandibular cavity is located close to the epidermis, in the same plane as the trigeminal nerve ganglion. The other head cavities, the premandibular and hyoid, are observed to be located more medially. In *S. torazame*, no additional head cavities develop rostral to the premandibular cavity (Fig. 2B).

As compared with stage III, the positions of the postotic branchiomeric nerve roots (IX, X) have shifted caudally on the rhombencephalon in stage IV (Fig. 2B). Because the glossopharyngeal nerve root is now located caudal to r6, this shift does not appear to result simply from the local growth of the hindbrain at the level of the otocyst.

The stage IV embryo also exhibits extensive neurite growth along the body. Numerous neurites are observed grow-

Fig. 1. Development of the nervous system of stage I and stage II *S. torazame* embryos. **A**: Lateral view of a stage I embryo (19-day, 3.5-mm). In the hindbrain, r2/3 and r3/4 boundaries are seen. Note that r3 is located dorsal to the first pharyngeal pouch. An otic placode (ot) is located lateral to r4. **B**: Whole-mount, stage I embryo immunochemically stained with anti-HNK-1 mAb. Note the specific staining of the mandibular head cavity (mnc) located rostral to the first pharyngeal pouch (pp1). The rostral boundary of r3 is seen on the neural tube. **C**: Scanning electron micrograph of a stage II embryo (22-day, 3.5-mm). Cephalic crest cells are colored green. Trigeminal crest cells (TC) are distributed rostral to the r2/3 boundary, hyoid crest cells (HC) adhere to r4, and another caudal cell population is emigrating from the caudal hindbrain. The crest cells are located superficial to the mesoderm, but the hyoid mesoderm (hm) is exposed between the trigeminal and hyoid crest cell populations. **D**: Another stage II *S. torazame* embryo. Compact crest cell sub-populations prefigure the cranial nerve primordia. The rostral cell population-the trigeminal nerve anlage (TC(V))-adheres proximally to r2 and bifurcates distally on both sides of the mandibular head cavity (mnc). The second cell population-the acusticofacial nerve anlage (HC(VII+VIII))-adheres to r4, and the third crest cell population-the glossopharyngeal nerve primordium (BC(IX))-adheres to r6. At this point, the otic pit (ot) is located at a level lateral to the r4/5 boundary. BC, branchial crest cells; br1, the first branchial arch; fb, forebrain; hb, hindbrain; HC, hyoid crest cells; hy, hyoid arch; hym, hyoid mesoderm; ma, mandibular arch; mb, midbrain; mnc, mandibular cavity; nt, notochord; opm, oropharyngeal membrane; ot, otic placode or pit; ov, optic vesicle; pp1and 2, pharyngeal pouches 1 and 2; prc, pericardial cavity; prcpl, prechordal plate; som, somites; sp, spiracle; TC, trigeminal crest cells; tra, truncus arteriosus. Bars, 200 μm.

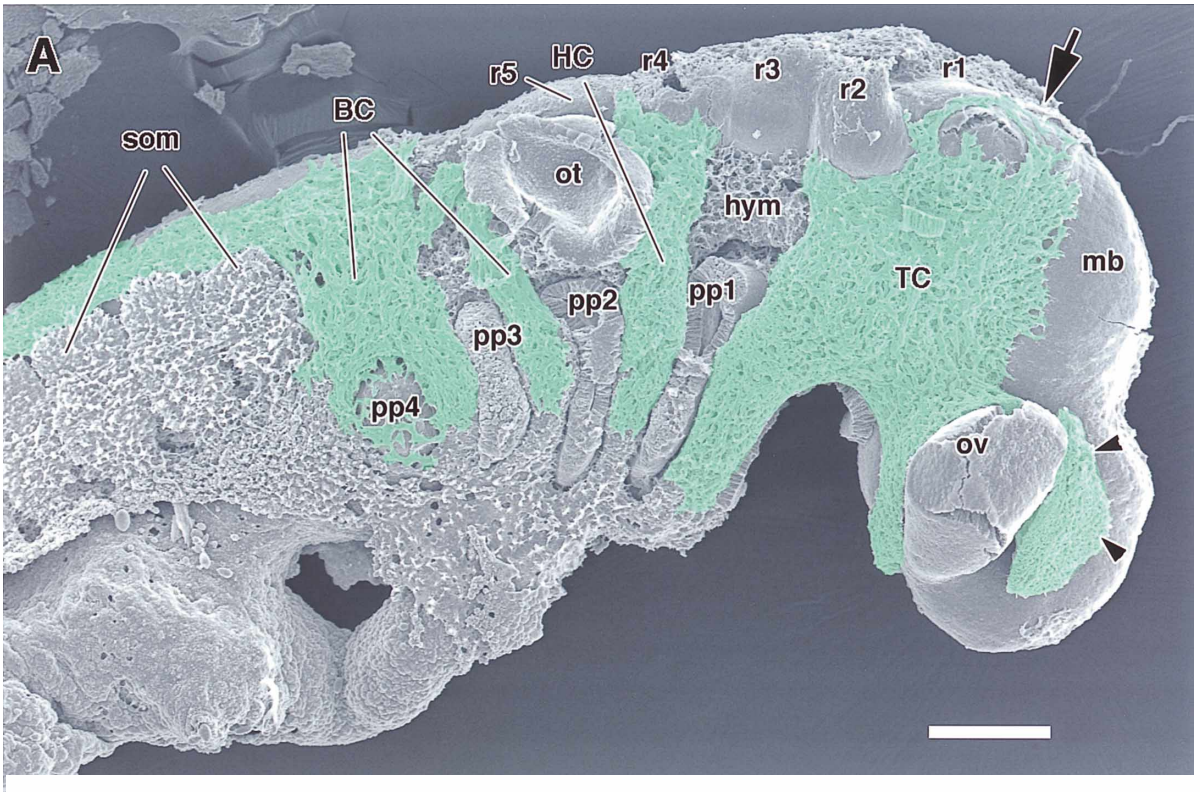

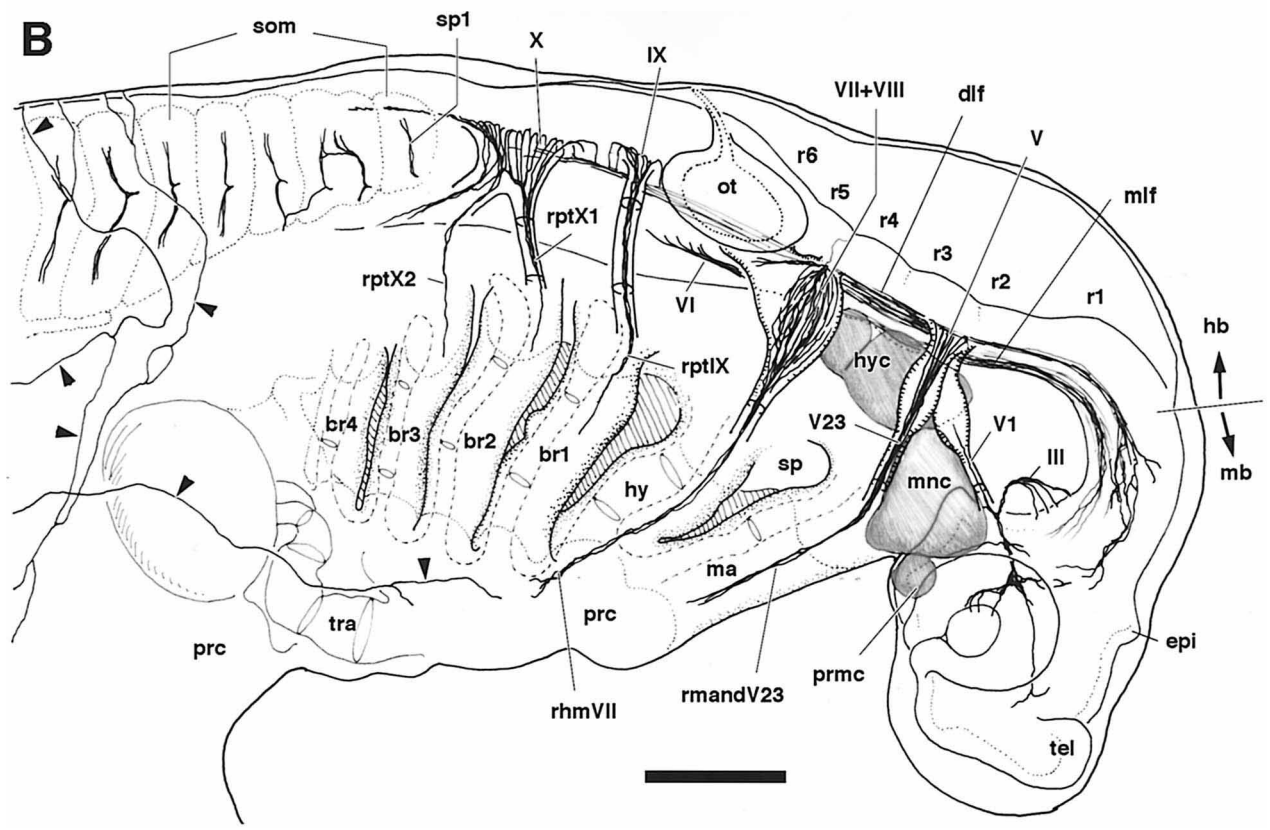

ing in an irregular pattern in the embryonic skin (Fig. 2B). These neurites belong to the Rohon-Beard cell class and have no morphological relationship to, or connection with, spinal nerves peripherally (see below). Moreover, in each branchiomeric nerve, the post-trematic branch seems to be the first to extend neurites (Fig. 2B).

Stage V (16- to 17-mm embryos)

By stage V, external gills have begun to develop on the caudal edges of hyoid and more caudal pharyngeal arches. The basic anatomical configuration of vertebrate peripheral nerves is emerging. Thus, the trigeminal nerve has grown neurites into the maxillary and mandibular regions, and the superficial ophthalmic branch grows from the preotic lateral line ganglion (Fig. 3A). Histological examination reveals that the contributions to the formation of the sensory ganglia made by the epibranchial placodes are similar to those in *Torpedo* embryos of the same body length (Froriep, 1891). A few epithelial placodal cells exhibit HNK-1-immunoreactivity, but acetylated tubulin immunoreactivity is associated exclusively with the cells within the ganglion (not shown). The trigeminal nerve root is found on r3, and the acusticofacial nerve root is on r4.

Graphic reconstruction of the head cavities from histological sections reveals typical topographical relationships with surrounding structures. The premandibular cavity is connected to its counterpart medially, between the hypothalamus and the hypophysis at the point where the rostral tip of the notochord attaches. Of the three cavities, the mandibular is located most laterally, between the ophthalmicus profundus and maxillomandibular branches of the trigeminal nerve; and the hyoid cavity is located medial to both the trigeminal and acusticofacial nerve roots (Fig. 3B, C). Moreover, the premandibular and hyoid cavities have connections with the oculomotor and abducens nerves, respectively (not shown). The trochlear nerve has not yet developed at this stage (Fig. 3A).

The overall anatomical configuration of the stage V S. *torazame* embryo is very similar to the 6.5-mm *Squalus acanthias* embryo described by Wedin (1955), the 12-mm Acanthias embryo described by Lamb (1902), and the stage K *Scyllium canicula* embryo described by Goodrich (1930). Thus, this pattern is apparently conserved among elasmobranch pharyngula.

Stage VI (53-day or 20- to 22-mm embryo)

The trochlear and olfactory nerves, as well as the posterior lateral line placode are visible by stage VI (Fig. 4A). The preotic lateral line ganglion has grown into a bipartite configuration: the buccal branch now grows from the ventral portion of the ganglion (buccal ganglion) into the maxillary region. In the brain, the appearance of nerve tract has made regionalization apparent. In addition to the mesencephalic trigeminal tract and the medial longitudinal and dorsolateral fasciculi, which have already been seen at stage IV (Fig. 2B), the tracts of the anterior, postoptic and habenular commissures, the dorsoventral diencephalic tract, the supraoptic tracts and the posterior commissure are all now present (Fig. 5). At this stage, the nerve tract morphology is comparable to that seen in late pharyngula of several other vertebrates including lampreys (Kuratani *et al*., 1998), teleosts (Chitnis *et al*., 1992), amphibia (Hartenstein, 1993; Burril and Easter, 1994), birds (Windle and Austin, 1936; Figdor and Stern, 1993), and mammals (Windle, 1970; Easter *et al*., 1993; reviewed by Kupffer, 1906).

As in the previous stage, the trigeminal and acusticofacial nerve roots are found on r3 and r4, respectively (Fig. 5A). These nerve roots are now located on the dorsolateral fasciculus, and direct contact between the crest cells and neurectoderm have long been lost (Fig. 6D, E; also see Fig. 2B). Epithelial head cavities retain the same topographical relationships as in the previous stage (Fig. 4B; compare with Fig. 3). Presumably, from the contribution made by the dorsolateral placodes to the preotic lateral line, the acusticofacial nerve complex is located far lateral to the trigeminal nerve. The topographical association between the head cavity and the cranial nerve is much closer between the trigeminal nerve and the mandibular cavity than between the acusticofacial nerve and the hyoid cavity, which are medio-laterally separated from each other (Fig. 4A, B).

Rohon-Beard neurites are still present in stage VI embryos (Fig. 6A, B, C). In the whole-mount stained embryos, these neurites are found to issue close to the midline of the neural tube (Fig. 6C). In most cases, HNK-1-positive, Rohon-Beard cell bodies are found within the neural tube (Fig. 6B), but in a few cases, cell bodies can also be found extra-

Fig. 2. Developmental morphology of the cranial nerves in stage III and stage IV *S. torazame* embryos. **A**: Scanning electron microphotograph of a stage III (8.0-mm) embryo. Cephalic crest cells are colored green. An arrow indicates the mid-hindbrain boundary. Rhombomeres 1 to 4 are recognized in the hindbrain. Note that the trigeminal crest cell population (TC) adheres to r2 and more anterior areas, and the hyoid crest cell population (HC) adheres to r4. As in the previous stage (Fig. 1C), the hyoid mesoderm (hym) is located between the trigeminal crest and hyoid crest cell populations. The hyoid cavity, which is not seen in this figure, is surrounded by mesodermal mesenchyme. Trigeminal crest cells are seen in the maxillary, mandibular and supraoptic (arrowheads) regions. The caudal population of cephalic crest cells (BC) have migrated into branchial arches, such that the cell sub-population in the first branchial arch is almost separated from the rest, prefiguring the morphology of the glossopharyngeal and vagus nerve primordia. **B**: Stage IV (9.5-mm) embryo stained with the anti-acetylated tubulin mAb. Immunoreactive neurites are surrounded by compact mesenchymal cells, which are presumably of crest origin. Post-trematic branches are recognized in some pharyngeal arches. Note that at this stage, the trigeminal nerve root (V) arises from r3, and the acusticofacial nerve root (VII+VIII) arises from the caudal portion of r4. Cranial nerve root-rhombomere relationships are ambiguous in the glossopharyngeal and vagus nerves. The three epithelial head cavities (prmc, mnc, hyc) are shaded. Of these, the mandibular cavity is located most superficially, between the profound ophthalmic (V1) and the mandibular (mandV23) branches of the trigeminal nerve. Arrowheads indicate early superficial neurites arising from Rohon-Beard cells in the trunk region. Bars, 500 μm.

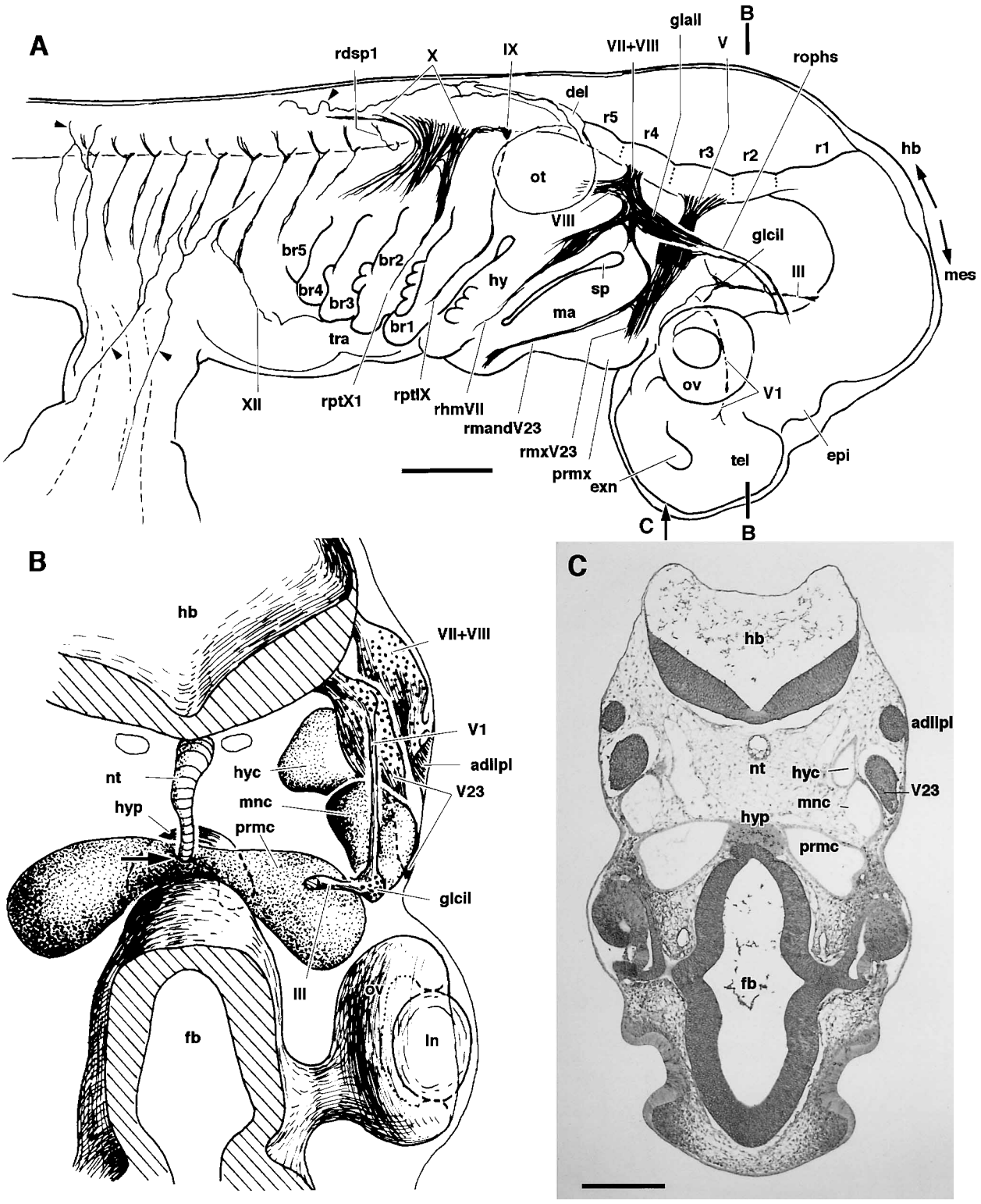

Fig. 3. Development of the peripheral nerve and head cavities at stage V. **A**: Left lateral view of an embryo stained with anti-acetylated tubulin mAb. An external nostril has appeared, and the telencephalon has enlarged. Note that the trigeminal nerve root is located on r3, and the acusticofacial nerve root is on r4. The region caudal to the thick lines labeled "B" was graphically reconstructed in panel B, while the arrow labeled "C" indicates the section shown in panel C. **B**: Graphic reconstruction of the head cavities in a stage V embryo. Of these, the most rostral premandibular cavity (prmc) is connected with its counterpart medially, caudal to the hypophysis (hyp), where the rostral tip of the notochord attaches (arrow). Note that the mandibular cavity lies close to the surface ectoderm between the ophthalmic profundus nerve (V1) and the maxillomandibular branch (V23) of the trigeminal nerve. **C**: Photomicrograph of a transverse section of a stage V embryo showing all three head cavities; the plane of the section is indicated by the arrow in panel A. Bars, 500 μm in A, 250 μm in C.

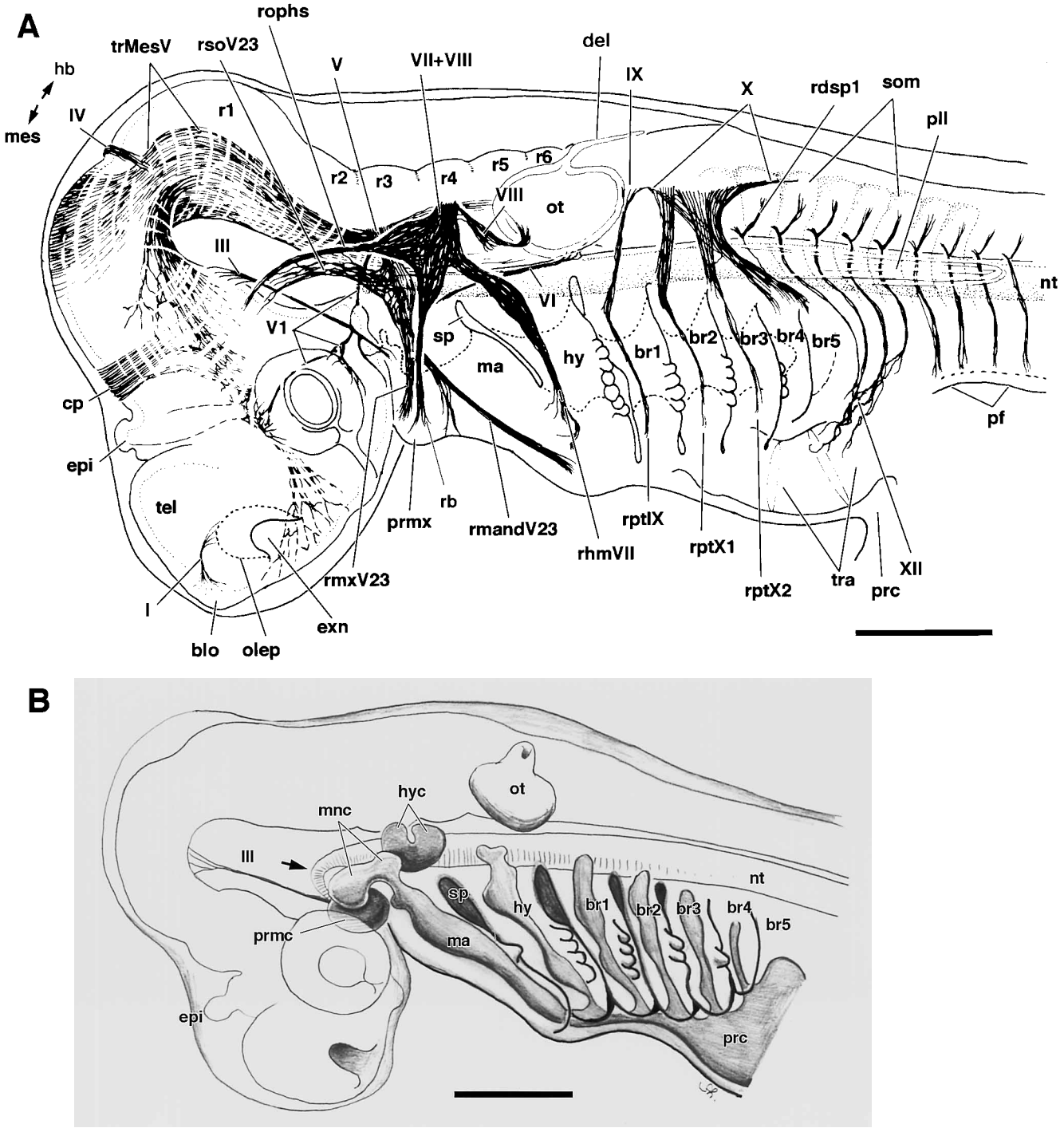

Fig. 4. Developmental morphology of the peripheral nervous system in stage VI *S. torazame* embryos. **A**: An embryo stained with the anti-acetylated tubulin mAb. The trigeminal nerve root, which now arises from r3, approaches the acusticofacial nerve root. **B**: Lateral view of a stage VI embryo. The oculomotor nerve has reached the premandibular cavity. The abducens nerve also contacts with the hyoid cavity, which is not reconstructed in this figure (see A). Graphic reconstruction of the head cavities is based on histological sections; only the mandibular cavity remains connected to the mandibular arch coelom. The arrow indicates the bending of the rostral notochord. Bars, 1 mm.

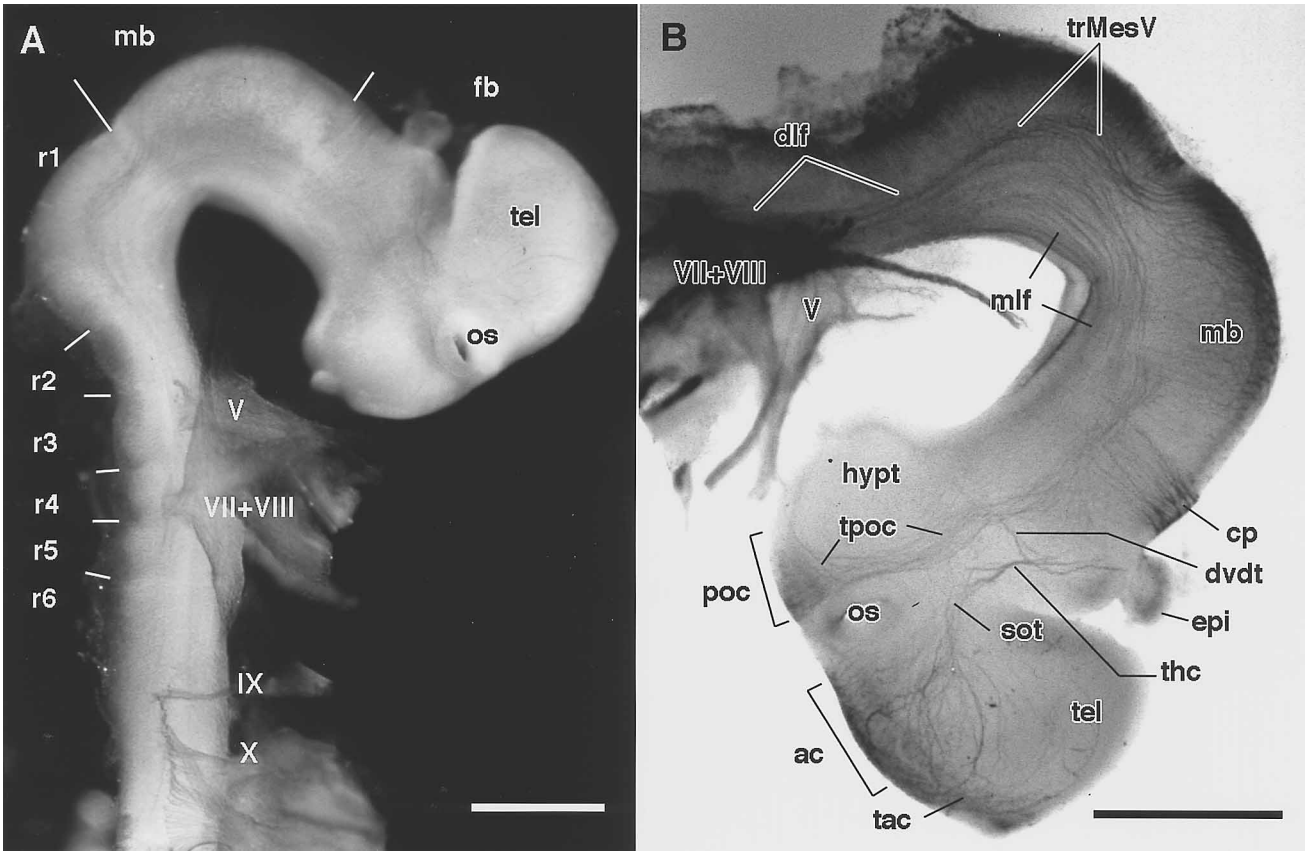

Fig. 5. Morphology of the CNS in *S. torazame* at stage V. **A**: The whole brain was dissected from the specimen shown in Fig. 4A. **B**: Enlargement of the same specimen seen in panel A. Note the development of nerve tracts in the various brain regions. ac, anterior commissure; cp, posterior commissure; dvdt, dorsoventral diencephalic tract; dlf, dorsolateral fasciculus; ep, epiphysis; fb, forebrain; mb, midbrain; mlf, medial longitudinal fasciculus; os, optic stalk; poc, postoptic commissure; r1–6, rhombomeres; sot, supraoptic tract; tac, tract of the anterior commissure; tel, telencephalon; thc, tract of the habenular commissure; tpoc, commissure of the postoptic tract; trMesV, mesencephalic trigeminal tract; V, VII+VIII, IX, X, branchiomeric nerve roots. Bars, 500 μm.

medullarly (Fig. 6C). Interestingly, the Rohon-Beard neurites do not supply the skin of the pectoral fin buds, which first become apparent at this stage (Fig. 6A). These neurites also invade the wall of the umbilical cord, a region never innervated by spinal nerve branches (Fig. 6A; also see Fig. 3A).

DISCUSSION

As a consequence of the macrolecithal nature of the development of embryos with umbilical cords, the shark pharyngula looks more like the pharyngula of an amniote embryo than that of a teleost or a lamprey embryo at a similar stage (Keibel, 1906). For example, the topographical relationship between the profundal nerve, the oculomotor nerve and the optic vesicle in the 9-mm *S. torazame* embryo is similar to that seen in the late pharyngula of amniotes (Keibel, 1906; Halley, 1955; Kuratani and Tanaka, 1990; Kuratani, 1997; Easter *et al.*, 1993). One might expect, therefore, that the morphotype of the elasmobranch embryo, formulated through vertebrate comparative embryology, is more directly representative than other embryos with morphotypes formulated on the basis of the anatomical features of the adult peripheral nerves (Tanaka, 1976, 1979; Tanaka and Nakao, 1979). However, a major difference is evident in the preotic region of the head, namely, the positions of the trigeminal and acusticofacial nerve roots, which appear to be associated with embryonic features unique to elasmobranchs. Importantly, the early pharyngula of *S. torazame* exhibits three cephalic crest cell populations extending from even-numbered rhombomeres to the superficial portion of the embryo. Thus, elasmobranch embryos exhibit the same head-specific, dorsolateral, crest cell migration pathways and the same conserved relationships with rhombomeres as are exemplified by amniote embryos (reviewed by Le Douarin *et al.*, 1984; and by Bronner-Fraser, 1995).

The branchiomeric nerves of vertebrates (e.g., chick: Tello, 1923; Lumsden and Keynes, 1989; Kuratani, 1991; *Lumsden et al.*, 1991; Niederländer and Lumsden, 1996; Lampetra: Kuratani *et al.*, 1998; Horigome *et al.*, 1999; reviewed by Kuhlenbeck, 1935; and by Gilland and Baker, 1993) characteristically develop on even-numbered rhombomeres. This is a consequence of the selective association of crest cells with those rhombomeres. Trigeminal crest cells adhere to r2, hyoid crest cells to r4, and branchial crest cells to r6 and further posterior. In amniote embryos, cephalic crest cells are known to be generated at all levels of the neuraxis, but are

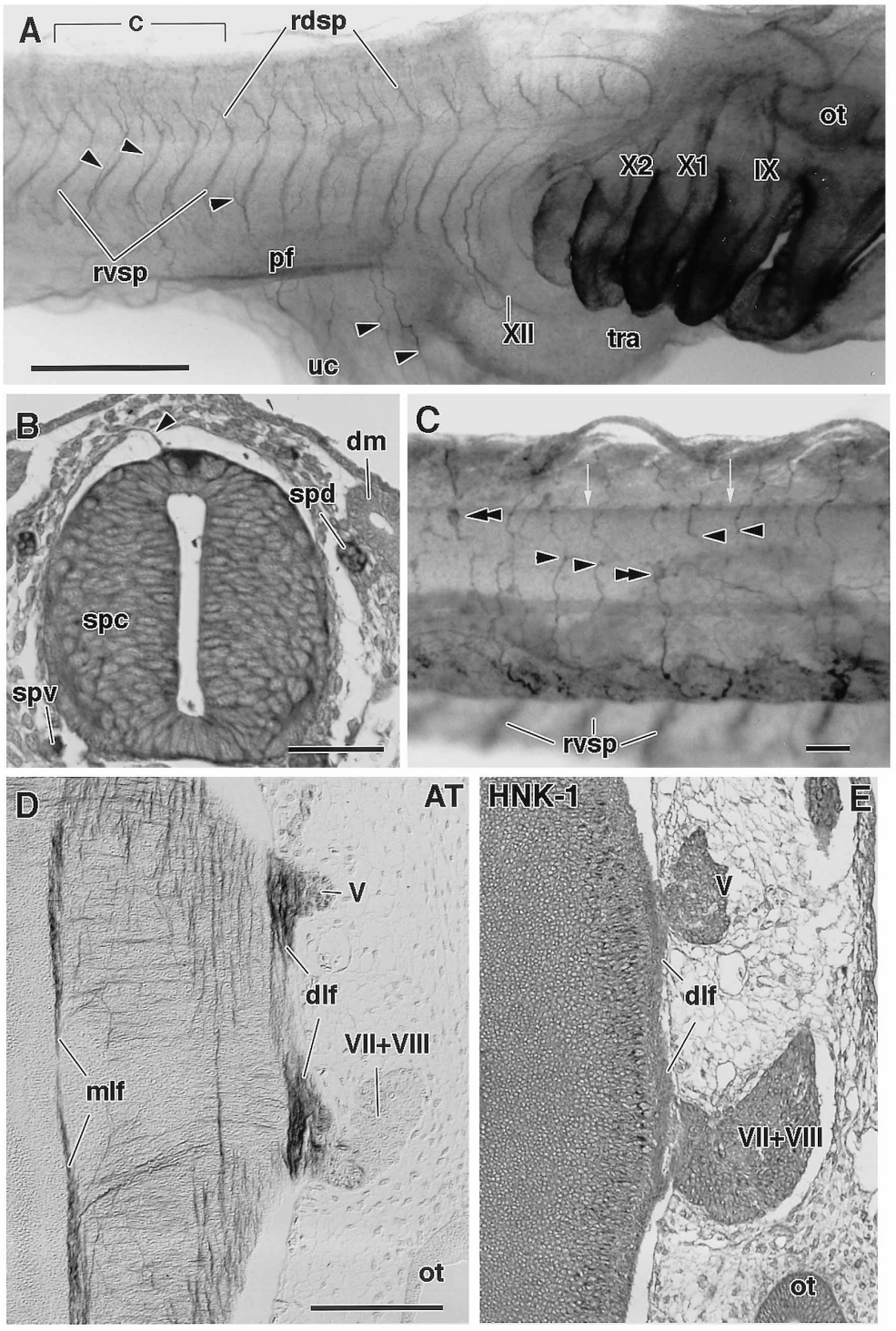

Fig. 6. Peripheral nerve development in stage IV and stage V embryos. **A**: Postotic region of a whole-mount embryo at stage V, stained immunohistochemically with the anti-acetylated tubulin mAb. Arrowheads indicate nerve processes belonging to Rohon-Beard cells. Note that these nerves do not develop in the pectoral fin bud (pf), but grow into the wall of the umbilical cord (uc). The region labeled "C" is enlarged and shown in panel C. **B**: Transverse section of a stage IV embryo, immunohistochemically stained with anti-HNK-1 mAb. Note an immunoreactive nerve process-a Rohon-Beard process-issues from the dorsal aspect of the neural tube in which the cell body is located. **C**: Enlarged dorsal view of the same embryo seen in panel A, showing Rohon-Beard neurites (arrows). White arrows indicate the dorsal medial line. Note that a few cell bodies are located outside the neural tube (double arrowheads). **D** and **E**: Two adjacent horizontal sections of a stage V embryo immunohistochemically stained with anti-acetylated tubulin (D) or anti-HNK-1 mAbs (E). At this stage, both the trigeminal and acusticofacial nerve roots (V, VII+VIII) arise from a thick nerve bundle in the hindbrain-the dorsolateral fasciculus (dlf). dm, dermomyotome; IX, glossopharyngeal nerve; mlf, medial longitudinal fasciculus; ot, otic vesicle; pf, pectoral fin bud; rdsp, spinal dorsal ramus; rvsp, spinal ventral ramus; spd, spinal dorsal root; spv, spinal ventral root; tra, truncus arteriosus; uc, umbilical cord; X1-2, vagus nerves. Bars, 1 mm in A, 200 μm in B to E.

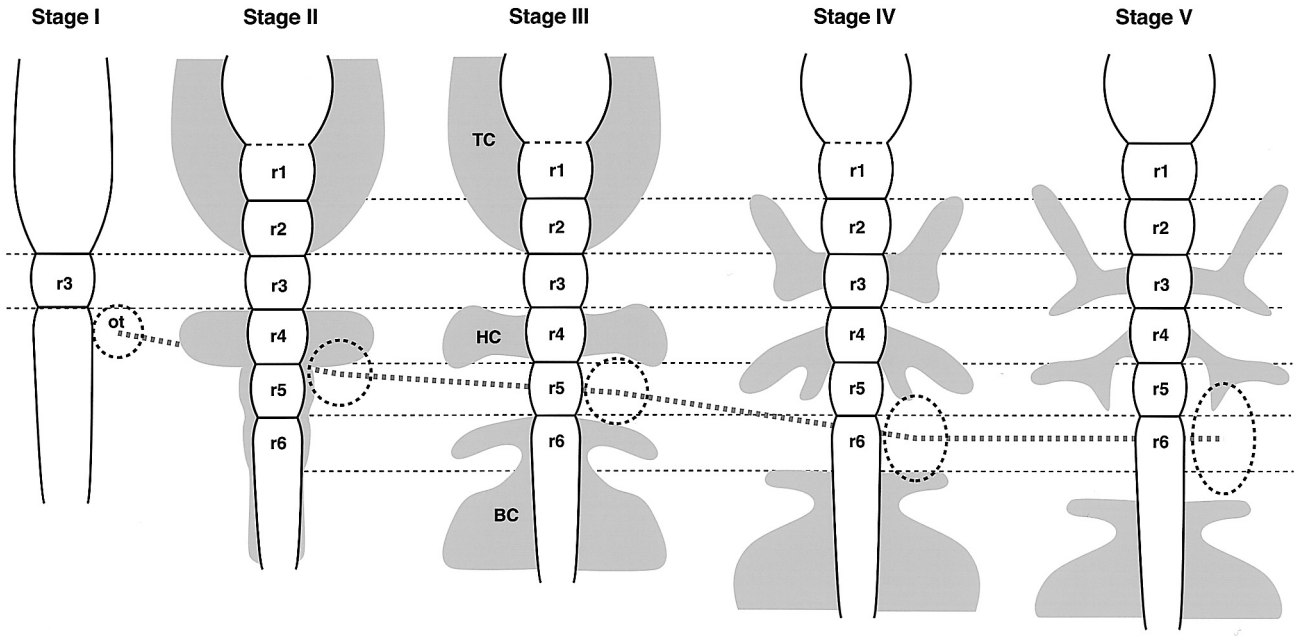

Fig. 7. Developmental changes in the relationships between the cranial nerve roots and the rhombomeres. Cranial nerve primordia are colored gray. No information was obtained for stage I in the present study. The anlagen are actually the crest cell populations (TC, HC, and BC cells) in stages II and III. Neural tubes are schematically illustrated, with each rhombomere arranged on the same horizontal level. Cephalic crest cells appear to emigrate from all levels of the neuraxis (r5 is associated with crest cells at stage II), and secondarily, two crest cell-free regions develop at the levels of r3 and r5 (stage III). This stage exhibits a phylotypic phase of the crest-rhombomere relationship conserved among other vertebrate embryos. Note that except for the acusticofacial nerve root, which remains on r4, all the cranial nerves shift caudally along the neuraxis through development. Additionally, note the caudal shift (indicated by a thick broken line) and enlargement of the otocyst. The latter seems to be responsible for the shift of the postotic nerves.

then secondarily excluded from the r3 and r5 levels (Serbedzija *et al*., 1992; Sechrist *et al*., 1993; Graham *et al*., 1993). Thus, the typical tri-population pattern of cephalic crest cells appears to be established in various vertebrate species including lampreys (Horigome *et al*., 1999), elasmobranchs (Froriep, 1891, 1902; Goodrich, 1918; de Beer, 1922), teleosts (Sadaghiani and Vielkind, 1990), amphibians (Froriep, 1917; Stone, 1926; Starck, 1963; Jacobson and Meier, 1984; Zackson and Steinberg, 1986; Hall and Hörstadius, 1988; Mayor *et al*., 1995; Northcutt and Brändle, 1995; Olsson and Hanken, 1996), reptiles (Meier and Packard, 1984), birds (Anderson and Meier, 1981; Kuratani and Kirby, 1991; Sechrist *et al*., 1993) and mammals (Halley, 1955; Müller and OíRahilly, 1980; Tan and Morriss-Kay, 1985; Maden *et al*., 1992; Osumi-Yamashita *et al*., 1994). Similar exclusion of crest cells from r5 is also apparent in *S. torazame* (Figs. 1C, 2A). The transient division of trigeminal crest cells into thalamic and trigeminal sub-populations (Scammon, 1911; and see Fig. 1C) raises the possibility that originally crest cells formed four cell populations rather than three. Trigeminal crest cell populations in lamprey embryos do not show such division, however (Horigome *et al*., 1999). Presumably, therefore, this feature is transient and may be specifically associated with elasmobranch embryos.

Segmental rhombomere-crest cell relationships serve as a critical developmental pre-pattern in branchiomeric nerve patterning. For example, in the chick embryo, heterotopic transplantation results in a re-patterning of the nerve roots that stands in contrast to spinal nerve metamerism, which primarily depends on somitic metamerism (Detwiler, 1934; Keynes and Stern, 1984; Rickmann *et al*., 1985; Tosney, 1987; Bronner-Fraser and Stern, 1991; Kuratani and Eichele, 1993). Moreover, adhesion of the trigeminal ganglionic primordium to the hindbrain is required for normal neuronal patterning and differentiation of the trigeminal nerve in the chick (Moody and Heaton, 1983a, b, c).

Epigenetic translocation of the cranial nerve roots

The present study confirms that, during development, the shark trigeminal nerve root shifts along the hindbrain neuraxis from r2 to r3. Similar aberrant morphologies have been described in several other elasmobranch embryos, in which the trigeminal nerve root was either found on r3 or was found too close to the root of the acusticofacial nerve, for example the 13-mm *Squalus acanthias* embryo (Neal, 1914) and, perhaps, the 12-mm *Torpedo ocellata* embryo (Froriep, 1905). However, as seen in various other vertebrates, in early pharyngula embryos of elasmobranch species, including *S. torazame*, the proximal portion of the trigeminal crest cell population (the trigeminal nerve primordium) attaches at a level corresponding to r2 or more anteriorly (*Torpedo ocellata*: Froriep, 1905; *Scyllium*: Goodrich, 1918; *Squalus acanthias*: Scammon, 1911; de Beer, 1922). This means that the shift in the position of the nerve roots along the brain stem is a secondary phenomenon that deviates from the vertebrate morphotype. This modification of the rhombomere-cranial nerve root relationship is illustrated in Fig. 7. The transposi-

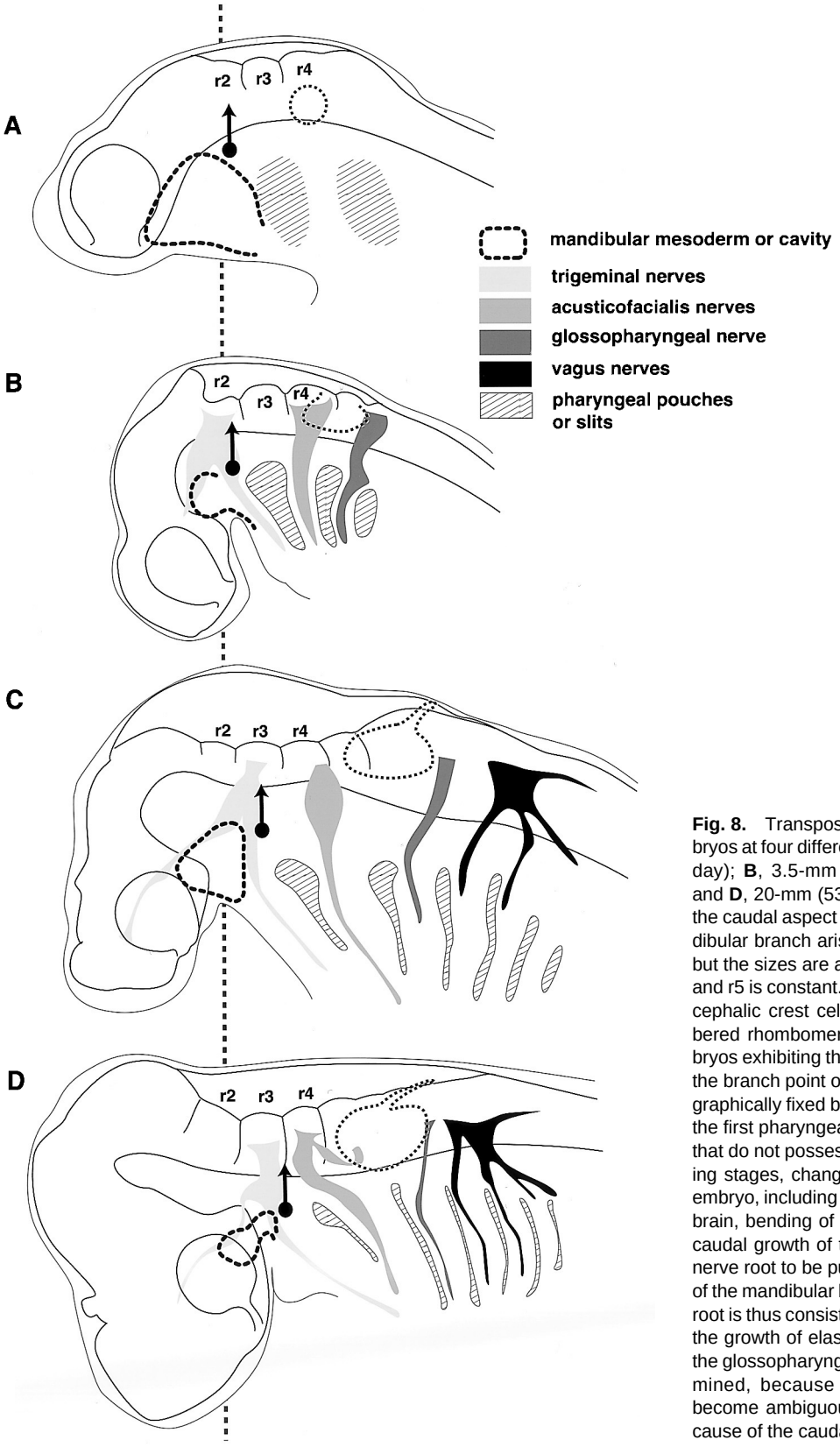

Fig. 8. Transposition of nerve roots in *S. torazame*. Embryos at four different stages are illustrated: **A**, 3.5-mm (19-day); **B**, 3.5-mm (22-day); **C**, 9.5-mm (age unknown); and **D**, 20-mm (53-day). In all the figures, arrows indicate the caudal aspect of the mandibular cavity where the mandibular branch arises. Embryos are not depicted at scale, but the sizes are adjusted so that the distance between r2 and r5 is constant. The earliest cranial nerve primordia-the cephalic crest cell sub-populations-adhere to even-numbered rhombomeres, as they do in other vertebrate embryos exhibiting the vertebrate phylotype (B). At this stage, the branch point of the mandibular branch is already topographically fixed between the mandibular cavity (mnc) and the first pharyngeal pouch, a situation not seen in animals that do not possess expanded head cavities. In the following stages, changes in the proportions of the developing embryo, including a relative increase in the size of the forebrain, bending of the cephalic flexure, and especially the caudal growth of the hypothalamus, cause the trigeminal nerve root to be pushed caudally relative to the fixed point of the mandibular branch. The caudal shift of the trigeminal root is thus consistent with the embryonic environment and the growth of elasmobranchs. The rhombomeric levels of the glossopharyngeal and vagus nerve roots are not determined, because the rhombomeric boundaries rapidly become ambiguous in the postotic hindbrain (C, D). Because of the caudal shift of the otic pit (the otocyst in older embryos) relative to the rhombomeres, as well as to the enlargement of the otocyst itself, these nerve roots may be caudally translocated along the hindbrain.

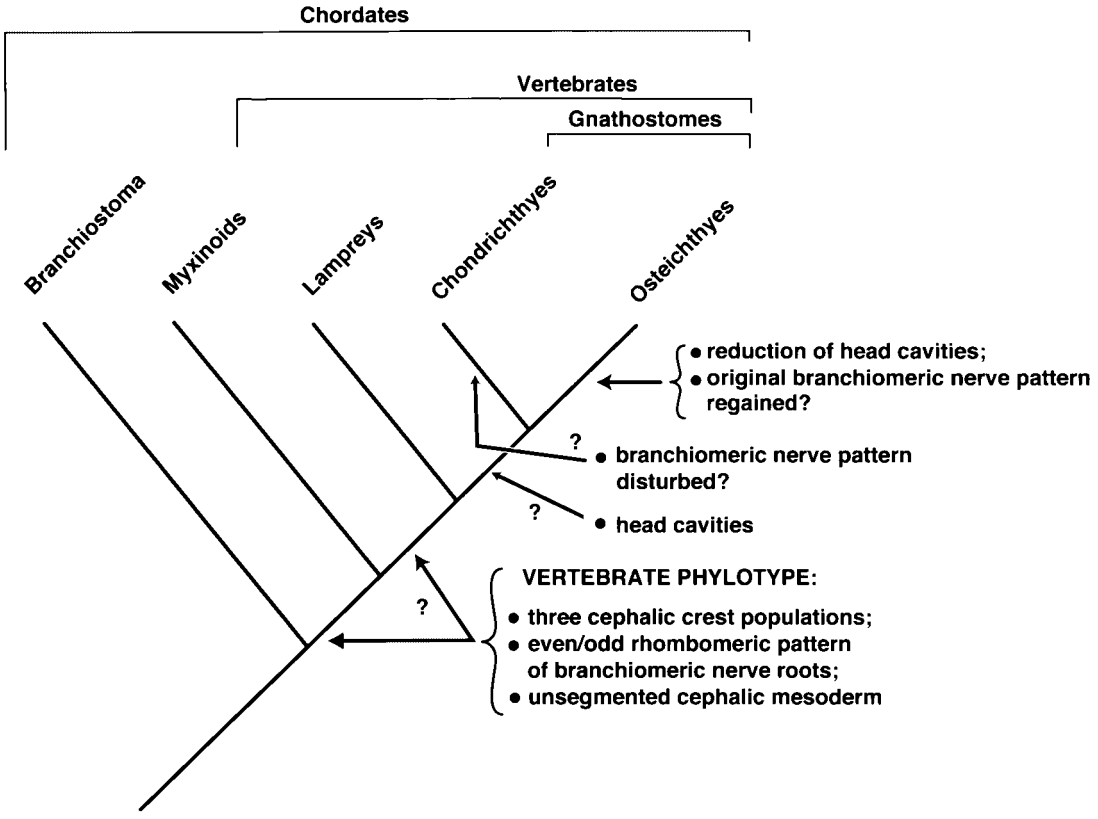

Fig. 9. Evolution of the morphological pattern of cranial nerve roots. The vertebrate phylotype was established before lampreys branched off. Since lampreys and amniotes, as well as early pharyngula of elasmobranchs, develop preotic branchiomeric nerve roots or their primordia on even-numbered rhombomeres (r2/4 pattern), this feature appears to represent a prototype of vertebrates. By contrast, the secondary shift of the nerve roots in elasmobranchs appears to have been acquired independently-the embryology of holocephalans is not well known. After the chondrichthyes branched off, the head cavities degenerated, and the r2/4 pattern of the cranial nerve roots, the original vertebrate phylotype, was regained.

tion of the trigeminal nerve root takes place between the 3.5-mm and the 9.0-mm stages in *S. torazame*. Histological observations reveal that the translocation takes place along the dorsolateral fasciculus, implying that the adhesion between the crest cell population and the hindbrain neurectoderm did not serve as a pre-pattern for the later anatomical configuration.

One possible explanation for the peculiar behavior of the trigeminal nerve root in elasmobranch embryos is that it is epigenetic in nature and may involve the unique feature of the elasmobranch pharyngula, namely, the head cavities. Among vertebrate groups, elasmobranch embryos develop enormously expanded head cavities during the pharyngula stages (Figs. 2, 3). Although epithelial head cavities are also observed in many gnathostome embryos, only in elasmobranchs do a complete set of cavities arise during development (see below). Important topographical relationships between the PNS and the head cavities are seen between the trigeminal nerve and the mandibular cavity. By the stage at which the trigeminal nerve anlage-the characteristic distribution pattern of the trigeminal crest cell population-is first visible, the primitive nerve root is found on r2 of the hindbrain and, distally, the cell streams are bifurcated dorsal to the expanding mandibular cavity (Fig. 1D). Of the two cell streams, the caudal stream corresponds to the site of mandibular branch development and is confined to a narrow space pressed between the caudal wall of the mandibular cavity and rostral wall of the first pharyngeal pouch. It is easy to imagine that the trigeminal nerve complex is continuously pulled caudally with respect to this fixed point as the proportions of the components of the head change, especially those changes resulting from caudal growth of the hypothalamus (Fig. 8). Also involved in this phenomenon would be the absence of a focal dorsolateral placode associated with the trigeminal nerve at these stages. In the facial nerve region, the preotic, antero-dorsal and antero-ventral dorsolateral placodes all contribute to branches associated with the acusticofacial nerve complex.

It is important to note that the morphological topography of the head cavities differ: the mandibular cavity is located superficially, and the other two develop medially (Goodrich, 1930). With dorso-laterally migrating cephalic crest cells paving the way, the branchiomeric nerve anlagen develop in the lateral part of the embryonic body. A close relationship, therefore, is established only between the trigeminal nerve and the mandibular cavity, which also explains the relatively stable position of the acusticofacial nerve root lying far lateral to the hyoid cavity.

A similar embryonic translocation of the nerve roots is

associated with the glossopharyngeal and vagus nerves: both nerves appear to shift caudally during development, perhaps as a result of being pushed in that direction by the enlarging otocyst (Figs. 7, 8). As already noted, this phenomenon is not due to the local growth of the hindbrain neurepithelium.

In conclusion, the early elasmobranch pharyngula with its odd/even pattern of rhombomeres and cranial nerve roots initially exhibits the characteristic vertebrate phylotype, but this pattern is secondarily lost in late pharyngula states. Presumably, the caudal translocation of the trigeminal nerve root may be of a secondary nature brought about by the presence of head cavities: a unique feature of elasmobranchs.

Evolutionary history of head cavities: a hypothetical scenario

According to the classical view of comparative embryology, selachian head cavities are equivalent to somites or myotomes in the trunk (reviewed by Goodrich, 1930; and by de Beer, 1937). It is indeed true that myogenesis from an epithelial state is reminiscent of the development of the myotome in the trunk. This has served as the basis for theories aimed at explaining the segmental organization of the vertebrate head (Bertmar, 1959; Jollie, 1977; Bjerring, 1977; reviewed by Goodrich, 1930; Jarvik, 1980; Jefferies, 1986; and by Gilland and Baker, 1993). Among known vertebrate groups, however, complete sets of clear and large epithelial cavities are restricted to elasmobranchs: pharyngula state lampreys do not possess mesodermal epithelial cavities (Damas, 1944; Horigome *et al*., 1999). Consequently, we are left with the question of whether these structures are primitive or acquired characteristics among vertebrates.

The occasional presence of vestigial head cavities in bony fishes and amniotes (Fraser, 1915; Wedin, 1949, 1952, 1953; Jacob *et al*., 1984; personal communication with Edwin Gilland; reviewed by Brachet, 1935) might infer that possession of these cavities is a shared, derived characteristic of gnathostomes that is secondarily diminished in the majority of members (Fig. 9). At the same time, the typical even/odd pattern of rhombomeres has been clearly established by the divergence of lampreys and gnathostomes (Horigome *et al*., 1999; Kuratani *et al*., 1999). The peculiar branchial nerve root morphology of elasmobranchs would thus represent a unique and derived character state caused by mandibular cavities remaining as epithelial structures of appreciable size for a long period during development.

One possible scenario that appears consistent with the above concept is that elasmobranchs maintain their head cavities because they are one of the earliest direct developers among vertebrates (with no larval stage), and thus need to differentiate extrinsic eye muscles extremely rapidly. Although no data are available on the development of the direct ancestors of elasmobranchs, extrinsic eye muscles do not appear at pharyngula stages in outgroups of gnathostomes. Hagfishes, a sister group of vertebrates, do not possess these eye muscles, nor do they seem to develop head cavities (Dean, 1899). Lampreys, another sister group of gnathostomes, on the other hand, possess a larval state that does not require a visual system or the rapid development of eye muscles. It has been speculated that lamprey extrinsic ocular muscles might originate in rostral myotomes (Neal, 1914, 1918; Damas, 1944; Bjerring, 1977; also see Hardisty and Rovainen, 1971). However, these myotomes are, in fact, postotic elements that have nothing to do with the preotic components of the head (Kuratani *et al*., 1997, 1999). The origin of the extrinsic ocular muscles in the lamprey is still unknown (Hardisty and Rovainen, 1971), although they do appear to arise before metamorphosis (unpublished personal observation in *Lampetra japonica*; see also Koltzoff, 1901).

As observed in sea urchins, which develop directly (without larval stages), acceleration of adult organogenesis involves rearrangement of cell lineages and embryonic primordia (reviewed by Wray and Raff, 1991; and by Wray, 1995). Elasmobranch head cavities may thus be embryonic structures primarily adaptive for accelerated eye muscle development and not mere vestigial metameric units of paraxial mesoderm. Similar concepts were presented by Adelmann (1926) and Wedin (1955), who assumed that the head cavities were an adaptation to accelerated head development in the shark. If the elasmobranch head cavities are adaptive anlagen for accelerated head development, and the apparent mesodermal segmentation of the head is merely an epigenetic secondary phenomenon (Starck, 1963; Kuratani *et al*., 1999), then cranial nerve morphology may have initially diverged from the pre-existing developmental plan of vertebrates, only to merge again later in those groups in which the cavities are diminished.

ACKNOWLEDGMENTS

We are grateful to Hisoka Hiruta and Koji Takada in Marine World Umino-Nakamichi, Fukuoka, for providing embryonic materials. We also thank Edwin Gilland for communicating his unpublished observations and valuable discussions. Sincere gratitude is extended to Shigenori Tanaka for his valuable comments on the manuscript. This work was supported by grants-in-aid from the Ministry of Education, Science and Culture of Japan.

REFERENCES

Adelmann HB (1926) The development of the premandibular head cavities and the relations of the anterior end of the notochord in the chick and robin. J Morphol 42: 371–439

Anderson CB, Meier S (1981) The influence of the metameric pattern in the mesoderm on migration of cranial neural crest cells in the chick embryo. Dev Biol 85: 385–402

Balfour FM (1878) The development of the elasmobranchial fishes. J Anat Physiol 11: 405–706

de Beer GR (1922) The segmentation of the head in *Squalus acanthias*. Quart J Microsc Sci 66: 457–474

de Beer GR (1937) "The Development of the Vertebrate Skull" Oxford University Press, London

Bertmar G (1959) On the ontogeny of the chordal skull in Characidae, with a discussion on the chondrocranial base and the visceral chondrocranium in fishes. Act Zool Stockholm 40: 203–364

Bjerring HC (1971) The nerve supply to the second metamere basicranial muscle in osteolepiform vertebrates, with some remarks on the basic composition of the endocranium. Act Zool Stockholm 52: 189–225

Bjerring HC (1977) A contribution to structural analysis of the head of craniate animals. Zool Script 6: 127–183
Brachet A (1935) "Traité d'Embryologie des Vertébrés" Masson & Cie, Etiteurs, Paris
Bronner-Fraser M (1995) Origins and developmental potential of the neural crest. Exp Cell Res 218: 405–417
Bronner-Fraser M, Stern C (1991) Effects of mesodermal tissues on avian neural crest cell migration. Dev Biol 143: 213–217
Burril JD, Easter SS Jr (1994) Development of the retinofugal projections in the embryonic and larval zebrafish (*Brachydario rerio*) J Comp Neurol 346: 583–600
Chitnis AB, Patel CK, Kim S, Kuwada JY (1992) A specific brain tract guides follower growth cones in two regions of the zebrafish brain. J Neurobiol 23: 845–854
Damas H (1944) Recherches sur le développement de *Lampetra fluviatilis* L. - contribution à l'étude de la cephalogénèse des vertébrés. Arch Biol (Paris) 55: 1–289
Dean B (1899) On the embryology of *Bdellostoma stouti*: A general account of myxinoid development from the egg and segmentation to hatching. Festschr. z. 70ten Geburst. v Kupffers. Jena: Gustav Fischer. pp 220–276
Detwiler SR (1934) An experimental study of spinal nerve segmentation in *Amblystoma* with reference to the plurisegmental contribution to the brachial plexus. J Exp Zool 67: 395–441
Dohrn A (1888) Studien zur Urgeschichte des Wirbeltierkörpers. Mitt a d Zool Stat Neapel 8–13
Easter SS Jr., Ross LS, Frankfurter A (1993) Initial tract formation in the mouse brain. J Neurosci 13: 285–299
Fraser EA (1915) The head cavities and development of the eye muscles in *Trichosurus vulpecula*, with notes on some other marsupials. Proc Zool Soc (London) 22: 299–346
Figdor MC, Stern CD (1993) Segmental organization of embryonic diencephalon. Nature 363: 630–634
Froriep A (1891) Entwicklungsgeschichte des Kopfes. Anat Heft 2: 561–605
Froriep A (1902) Zur Entwicklungsgeschichte des Wirbeltierkopfes. Verh Anat Ges 1902: 34–46
Froriep A (1905) Die occipitalen Urwirbel der Amnioten im Vergleich mit denen der Selachier. Verh Anat Ges 1905: 111–120
Froriep A (1917) Die Kraniovertebralgrenze bei den Amphibien .*Salamandra atra*). Beitrag zur Entwicklungsgeschichte des Wirbeltierkopfes. Arch Anat Physiol 191: 761–102
Gilland E, Baker R (1993) Conservation of neuroepithelial and mesodermal segments in the embryonic vertebrate head. Act Anat 148: 110–123
Goodrich ES (1918) On the development of the segments of the head in *Scyllium*. Quart J Microsc Sci 63: 1–30
Goodrich ES (1930) "Studies on the Structure and Development of Vertebrates" McMillan, London
Graham A, Heyman I, Lumsden A (1993) Even-numbered rhombomeres control the apoptotic elimination of neural crest cells from odd-numbered rhombomeres in the chick hindbrain. Development 119: 233–245
Hall BK, Hörstadius S (1988) "The Neural Crest" Oxford University Press, New York
Halley G (1955) The placodal relations of the neural crest in the domestic cat. J Anat 89: 133–152
Hardisty MW, Rovainen CM (1971) Morphological and functional aspects of the muscular system. In: "The Biology of Lampreys" (MW Hardisty, IC Potter eds) Vol 4, Academic Press, London, pp 137–231
Hartenstein V (1993) Early pattern of neuronal differentiation in the *Xenopus* embryonic brainstem and spinal cord. J Comp Neurol 328: 213–231
Horigome N, Myojin M, Ueki T, Hirano S, Aizawa S, Kuratani S (1999) Development of cephalic neural crest cells in embryos of a cyclostome, *Lampetra japonica*, with special reference to the evolution of the jaw. Dev Biol 207: 287–308
Jacob M, Jacob HJ, Wachtler F, Christ B (1984) Ontogeny of avian extrinsic ocular muscles. I. A light- and electron-microscopic study. Cell Tiss Res 237: 549–557
Jacobson AG. and Meier S (1984) Morphogenesis of the head of the newt: mesodermal segments, neuromeres, and distribution of neural crest. Dev Biol 106: 181–193
Jarvik E (1980) "Basic Structure and Evolution of Vertebrates" Vol 2, Academic Press, New York
Jefferies RPS (1986) "The Ancestry of the Vertebrates" British Museum (Natural History), London
Jollie MT (1977) Segmentation of the vertebrate head. Am Zool 17: 323–333
Keibel F (1906) Die Entwickelung der Äusseren Körperform der Wirbeltierembryonen, insbesondere der menschlichen Embryonen aus den ersten 2 Monaten. In "Handbuch der vergleichenden und experimentellen Entwickelungsgeschichte der Wirbeltiere" (O Hertwig ed.) 1ster Band, 2ter Teil, Gustav Fischer, Jena, pp 1–176
Keynes RJ, Stern CD (1984) Segmentation in the vertebrate nervous system. Nature 310: 786–789
Koltzoff NK (1901) Entwicklungsgeschichte des Kopfes von *Petromyzon planeri*. Bull Soc Nat Moscou 15: 259–589
Kuhlenbeck H (1935) Über die morphologische Bewertung der sekundären Neuromerie. Anat Anz 81: 129–148
von Kupffer K (1906) Die Morphologie des Centralnervensystems. In "Handbuch der vergleichenden und experimentellen Entwickelungsgeschichte der Wirbeltiere" (O Hertwig ed.) Bd. 2, 3 ter Theil, Gustav Fischer, Jena. pp 1–272
Kuratani SC (1991) Alternate expression of the HNK-1 epitope in rhombomeres of the chick embryo. Dev Biol 144: 215–219
Kuratani S (1997) Spatial distribution of postotic crest cells defines the head/trunk interface of the vertebrate body: embryological interpretation of peripheral nerve morphology and evolution of the vertebrate head. Anat Embryol 195: 1–13
Kuratani SC, Eichele G (1993) Rhombomere transplantation repatterns the segmental organization of cranial nerves and reveals cell-autonomous expression of a homeodomain protein. Development 117: 105–117
Kuratani SC, Kirby ML (1991) Initial migration and distribution of the cardiac neural crest in the avian embryo: An introduction to the concept of the circumpharyngeal crest. Am J Anat 191: 215–227
Kuratani S, Tanaka S (1990) Peripheral development of avian trigeminal nerves. Am J Anat 187: 65–80
Kuratani S, Ueki T, Aizawa S, Hirano S (1997) Peripheral development of the cranial nerves in a cyclostome, *Lampetra japonica*: morphological distribution of nerve branches and the vertebrate body plan. J Comp Neurol 384: 483–500
Kuratani S, Horigome N, Ueki T, Aizawa S, Hirano S (1998) Stereotyped axonal bundle formation and neuromeric patterns in embryos of a cyclostome, *Lampetra japonica*. J Comp Neurol 391: 99–114
Kuratani S, Horigome N, Hirano S (1999) Developmental morphology of the cephalic mesoderm and re-evaluation of segmental theories of the vertebrate head: evidence from embryos of an agnathan vertebrate, *Lampetra japonica*. Dev Biol 210: 381–400
Lamb AB (1902) The development of the eye muscles in *Acanthias*. Am. J. Anat. 1: 185–202.
Le Douarin NM, Cochard P, Vincent M, Duband JL, Tucker GC, Teillet MA, Thiery JP (1984) Nuclear, cytoplasmic, and membrane markers to follow neural crest cell migration: a comparative study. In "The Role of Extracellular Matrix in Development" (Trelstad RL, ed) Alan R. Liss, Inc., New York, pp 373–398
Lumsden A, Keynes R (1989) Segmental patterns of neuronal development in the chick hindbrain. Nature 337: 424–428
Lumsden A, Sprawson N, Graham A (1991) Segmental origin and

migration of neural crest cells in the hindbrain region of the chick embryo. Development 113: 1281–1291
Maden A, Horton C, Graham A, Leonard L, Pizzey J, Siegenthaler G, Lumsden A, Eriksson U (1992) Domains of cellular retinoic acid-binding protein I (CRABP I) expression in the hindbrain and neural crest of the mouse embryo. Mech Dev 37: 13–27
Mallat J (1996) Ventilation and the origin of jawed vertebrates: a new mouth. Zool J Linn Soc 117: 329–404
Marshall AM (1881) On the head cavities and associated nerves of elasmobranchs. Quart J Microsc Sci 21: 72- (cited in Goodrich, 1918)
Mayor R, Morgan R, Sargent M (1995) Induction of the prospective neural crest of *Xenopus*. Development 121: 767–777
Meier S, Packard DS Jr (1984) Morphogenesis of the cranial segments and distribution of neural crest in embryos of the snapping turtle, *Chelydra serpentina*. Dev Biol 102: 309–323
Moody SA, Heaton MB (1983a) Developmental relationships between trigeminal motoneurons in chick embryos. I. Ganglion development is necessary for motoneuron migration. J Comp Neurol 213: 327–343
Moody SA, Heaton MB (1983b) Developmental relationships between trigeminal motoneurons in chick embryos. II. Ganglion axon ingrowth guides motoneuron migration. J Comp Neurol 213: 344–349
Moody SA, Heaton MB (1983) Developmental relationships between trigeminal ganglia and trigeminal motoneurons in chick embryos. III. Ganglion perikarya direct motor axon growth in the peripherie. J Comp Neurol 213: 350–364
Müller F, OíRahilly R (1980) Early development of the nervous system in staged insectivore and primate emrbyos. J Comp Neurol 193: 741–751
Neal HV (1914) Morphology of the eye muscle nerves. J Morphol 25: 1–186
Neal HV (1918a) Neuromeres and metameres. J Morphol 31: 293–315
Neal HV (1918b) History of eye muscles. J Morphol 30: 433–453
Neal HV, Rand HW (1942) “Comparative Anatomy” The Blakiston Co, Philadelphia
Niederländer C, Lumsden A (1996) Late emigrating neural crest cells migrate specifically to the exit points of cranial branchiomotor nerves. Development 122: 2367–2374
Norris HW, Hughes SP (1920) The cranial, occipital, and anterior spinal nerves of the dogfish, *Squalus acanthias*. J Comp Neurol 31: 293–398
Northcutt RG (1993) A reassessment of Goodrichís model of cranial nerve phylogeny. Act Anat 148: 71–80
Northcutt RG (1997) Evolution of gnathostome lateral line ontogenies. Brain Behav Evol 50: 25–37
Northcutt RG, Brändle K (1995) Development of branchiomeric and lateral line nerves in the axolotl. J Comp Neurol 355: 427–454
Olsson L, Hanken J (1996) Cranial neural-crest migration and chondrogenic fate in the oriental fire-bellied toad *Bombina orientalis*: defining the ancestral pattern of head development in anuran amphibians. J Morphol 229: 105–120
Osumi-Yamashita N, Ninomiya Y, Doi H, Eto K (1994) The contribution of both forebrain and midbrain crest cells to the mesenchyme in the frontonasal mass of mouse embryos. Dev Biol 164: 409–419
Platt JB (1891) A contribution to the morphology of the vertebrate head, based on a study of *Acanthias vulgaris*. J Morphol 5: 79–106
Rickmann M, Fawcett J, Keynes RJ (1985) The migration of neural crest cells and the growth of motor axons through the rostral half of the chick somite. J Embryol Exp Morphol 90: 437–455
Sadaghiani B, Vielkind JR (1990) Distribution and migration pathways of HNK-1-immunoreactive neural crest cells in teleost fish embryos. Development 110: 197–209
Scammon RE (1911) Normal plates of the development of *Squalus acanthias*. Keibelís Normaltafeln zur Entwicklungsgeschichte der Wirbeltiere. 12: 1–140
Sechrist J, Serbedzija GN, Sherson T, Fraser S, Bronner-Fraser M (1993) Segmental migration of the hindbrain neural crest does not arise from segmental generation. Development 118: 691–703
Serbedzija GN, Bronner-Fraser M, Fraser SE (1992) Vital dye analysis of cranial neural crest cell migration in the mouse. Development 116: 297–307
Starck D (1963) Die Metamerie des Kopfes der Wirbeltiere. Zool Anz 170: 393–428
Stone LS (1926) Further experiments on the extirpation and transplantation of mesectoderm in *Amblystoma punctatum*. J Exp Zool 44: 95–131
Tan SS, Morriss-Kay GM (1985) The development and distribution of the cranial neural crest in the rat embryo. Cell Tiss Res 240: 403–416
Tanaka S (1976) Facial nerve of the shark (*Mustelus manazo*) and its comparison with the glossopharyngeal nerve. Act Anat Nippon 51: 1–16
Tanaka S (1979) Makroscopische Untersuchung des Nervus glossopharyngeus der Haifische (*Mustelus manazo*) Anat Anz 146: 456–469
Tanaka S, Nakao T (1979) A macroscopical study of the vagal nerve of sharks (*Mustelus manazo*) with special reference to morphological features of its branchial branches (in Japanese) Act Anat Nippon 54: 307–321
Tello JF (1923) Les différenciations neuronales dans l’embryon du poulet pendent les premiers jours de l’incubation. Trav Lab Invest Biol Univ Madrid 21: 1–93
Tosney KW (1987) Proximal tissues and patterned neurite outgrowth at the lumbosacral level of the chick embryo: deletion of the dermamyotome. Dev. Biol 122: 540–558
Wedin B (1949) The development of the head cavities in *Alligator mississippiensis* Daud. Lunds Univ. Arssikr. N. F. avs. 2, 45: 1–32 (cited in Starck, 1963)
Wedin B (1952) Tissue bridges and tubular connections between the premandibular cavities and Rathkes pouch. Proc. Koninkl. Akad. v. Wetensch. Amsterdam C55: 416–428 (cited in Starck, 1963)
Wedin B (1953) The development of the head cavities in *Ardea cinerea L*. Act Anat 17: 240–252
Wedin B (1955) Embryonic segmentations in the head. Malmö, (cited in Starck, 1963)
Wilson SW, Ross LS, Parret T, Easter SS (1990) The development of a simple scaffold of axon tracts in the brain of the embryonic zebrafish, *Brachydanio rerio*. Development 108: 121–145
Windle W (1970) Development of neural elements in human embryos of four to seven weeks gestation. Exp Neurol Suppl 5: 44–83
Windle WF, Austin MF (1936) Neurofibrillar development in the central nervous system of chick embryos up to 5 days of incubation. J Comp Neurol 63: 431–463
van Wijhe JW (1882) Über die Mesodermsegmente und die Entwicklung der Nerven des Selachierkopfes. Ver. Akad. Wiss. Amsterdam, Groningen, pp 1–50
Wray GA (1995) Punctuated evolution of embryos. Science 267: 1115–1116
Wray GA, Raff R (1991) The evolution of developmental strategy in marine invertebrates. TREE 6: 45–50
Zackson SL, Steinberg MS (1986) Cranial neural crest cells exhibit direct migration on the pronephric duct pathway: further evidence for an in vivo adhesion gradient. Dev Biol 117: 342–353

(Received February 19, 2000 / Accepted April 15, 2000)